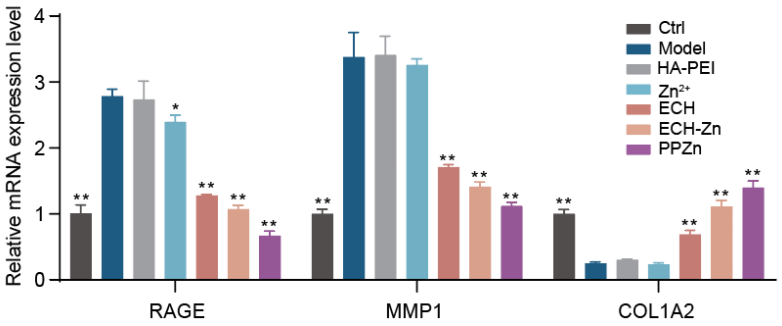

Figure S1 qRT-PCR detection of RAGE, MMP1 and COL1A2 mRNA levels in HaCaT cells after indicated treatment. *$P < 0.05$, **$P < 0.01$, compared with model.

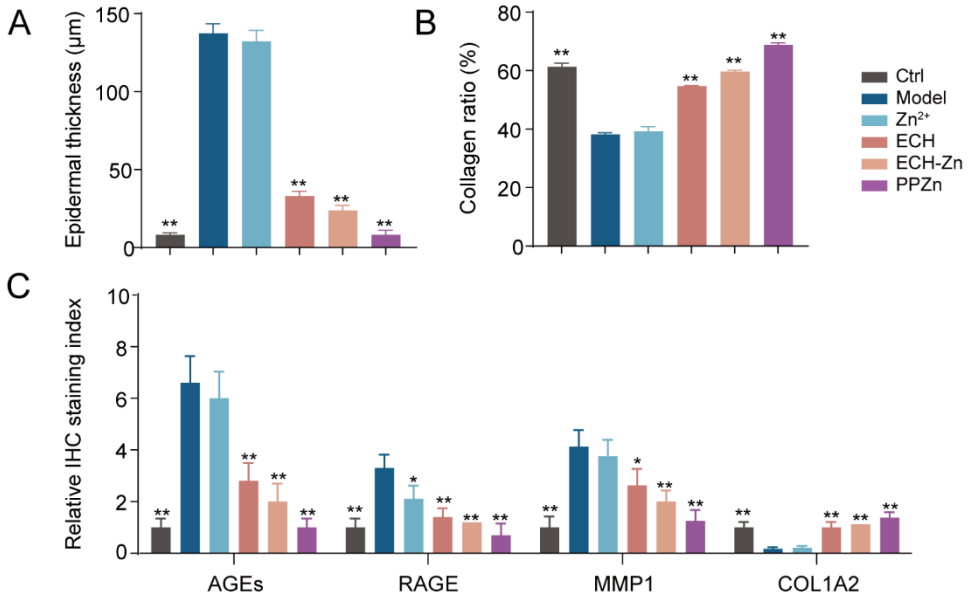

Figure S2 Statistical graph of skin epidermal thickness (A), collagen ratio (B), and relative IHC staining index (C) in mice. *$P < 0.05$, **$P < 0.01$, compared with model.

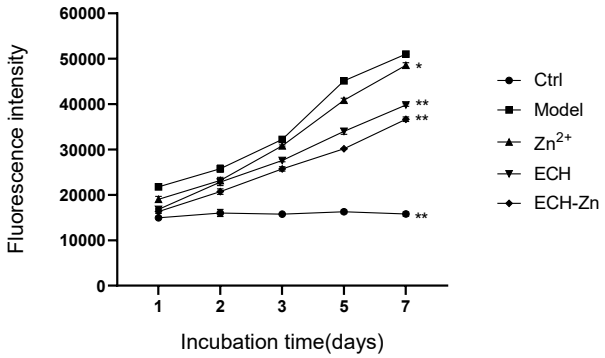

Figure S3 Effects of Zn^{2+}, ECH and ECH-Zn on the formation of AGEs in BSA-MGO system. **$P < 0.01$, compared with model.

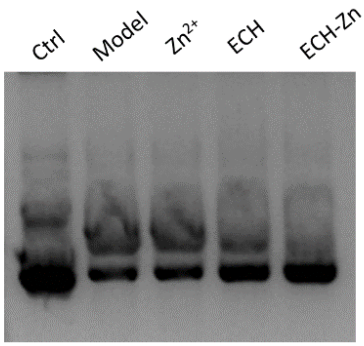

Figure S4 Electropherogram of MGO damaged DNA (plasmid: PGL3-Basic) inhibited by Zn^{2+}, ECH and ECH-Zn.

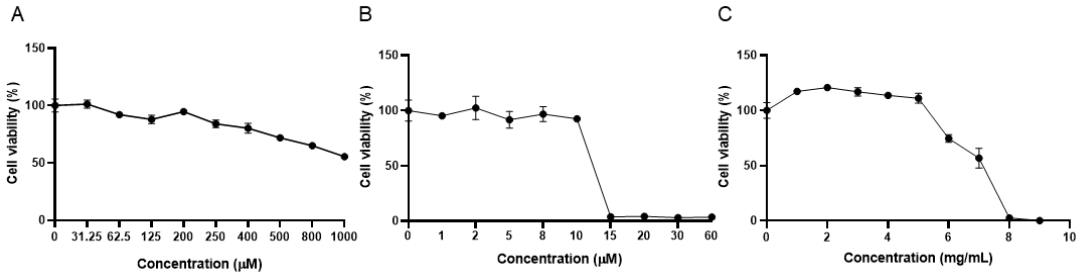

Figure S5 CCK8 results for ECH (A), Zn^{2+} (B), and PPZn (C). Left: ECH; Right: PPZn.

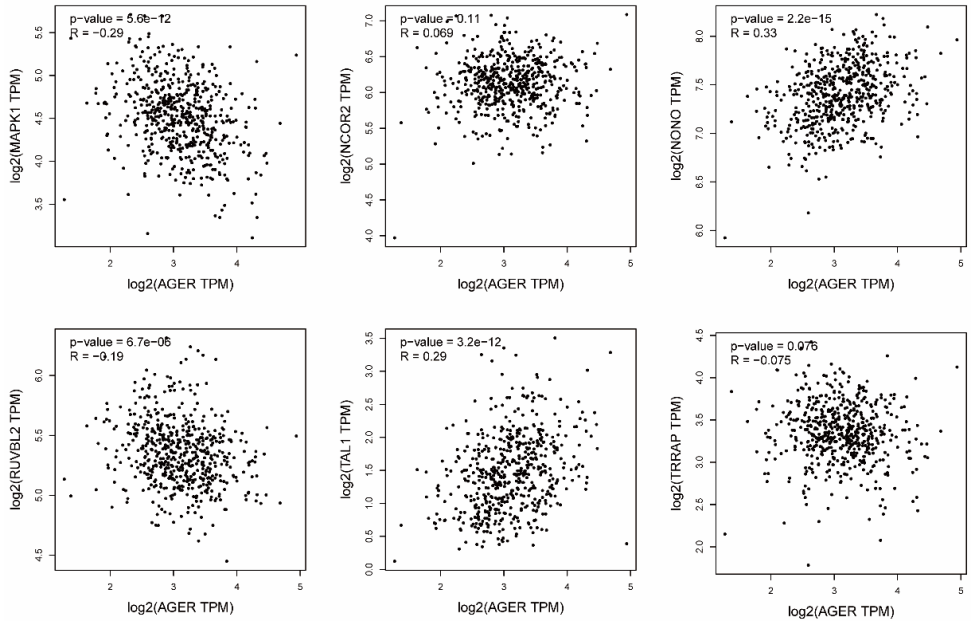

Figure S6 Correlation analysis between *MAPK1*, *NCOR2*, *NONO*, *RUVBL2*, *TAL1* or *TRRAP*, and *AGER* in skin was performed using GEPIA2 web server.

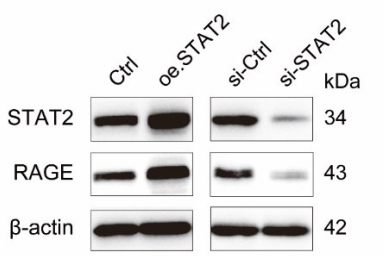

Figure S7 Western blot analysis of STAT2, RAGE and β-actin protein levels in HaCaT cells after indicated treatment.

Table S1. Plasmid information.

Plasmid	Source
pcDNA3.1-MDM2 plasmid	unibio
pcDNA3.1-STAT2 plasmid	unibio
PRL-TK plasmid	Tsingke
PGL3-Basic plasmid	Tsingke
RAGE promoter plasmid	Tsingke

Table S2. Sequences of siRNA.

Gene	Sequence
Species: Human	
si-STAT2-Sense	GGCUGACUUCACUAAGCGA (dT)(dT)
si-STAT2-Antisense	UCGCUUAGUGAAGUCAGCC (dT)(dT)

Table S3. Sequences of qRT-PCR primers.

Gene	Sequence
Species: Human	
GAPDH-Foward	GTCTCCTCTGACTTCAACAGCG
GAPDH-Reverse	ACCACCCTGTTGCTGTAGCCAA
RAGE-Foward	CACCTTCTCCTGTAGCTTCAGC
RAGE-Reverse	AGGAGCTACTGCTCCACCTTCT
MDM2-Foward	TGTTTGGCGTGCCAAGCTTCTC
MDM2-Reverse	CACAGATGTACCTGAGTCCGATG
Species: Mouse	
GAPDH-Foward	GTCTCCTCTGACTTCAACAGCG
GAPDH-Reverse	ACCACCCTGTTGCTGTAGCCAA
RAGE-Forward	GCCACTGGAATTGTCGATGAGG
RAGE-Reverse	GCCACTGGAATTGTCGATGAGG